Disassociated molecular orientation distributions of a composite cellulose–lignin carbon fiber precursor: A study by rotor synchronized

Carbohydrate Polymers 254 (2021) 117293

Contents lists available at ScienceDirect

Carbohydrate Polymers

journal homepage: www.elsevier.com/locate/carbpol

Disassociated molecular orientation distributions of a composite cellulose–lignin carbon fiber precursor: A study by rotor synchronized NMR spectroscopy and X-ray scattering

Leo Svenningsson [a], Jenny Bengtsson [b], Kerstin Jedvert [b], Werner Schlemmer [c], Hans Theliander [a,d], Lars Evenäs [a,d,*]

[a] Department of Chemistry and Chemical Engineering, Chalmers University of Technology, Göteborg, Sweden
[b] Materials and Production, RISE IVF Research Institutes of Sweden, Mölndal, Sweden
[c] Institute of Bioproducts and Paper Technology, Graz University of Technology, Graz, Austria
[d] Wallenberg Wood Science Center, Göteborg, Sweden

ARTICLE INFO

Keywords:
Carbon fibers
Lignin
Regenerated cellulose
Rotor synchronized magic-angle spinning
Molecular orientation distribution
Fiber
Wood
Solid-state NMR
X-ray scattering
Composite

ABSTRACT

Cellulose–lignin composite carbon fibers have shown to be a potential environmentally benign alternative to the traditional polyacrylonitrile precursor. With the associated cost reduction, cellulose–lignin carbon fibers are an attractive light-weight material for, e.g. wind power and automobile manufacturing. The carbon fiber tenacity, tensile modulus and creep resistance is in part determined by the carbon content and the molecular orientation distribution of the precursor. This work disassociates the molecular orientation of different components in cellulose–lignin composite fibers using rotor-synchronized solid-state nuclear magnetic resonance spectroscopy and X-ray scattering. Our results show that lignin is completely disordered, in a mechanically stretched cellulose–lignin composite fiber, while the cellulose is ordered. In contrast, the native spruce wood raw material displays both oriented lignin and cellulose. The current processes for fabricating a cellulose–lignin composite fiber cannot regain the oriented lignin as observed from the native wood.

1. Introduction

There is currently a growing aspiration of producing inexpensive carbon fibers, mainly to achieve a suitable light-weight material for the automotive and wind power industry (Mainka et al., 2015). As of now, carbon fibers are mainly produced from polyacrylonitrile (PAN), an expensive and fossil-based precursor, which limits extensive use of composites reinforced with carbon fibers (Baker & Rials, 2013). Therefore, alternative precursor materials are continuously being investigated. Frank, Steudle, Ingildeev, Spörl, and Buchmeiser (2014) have summarized the properties that are required of a polymer to be considered as a good precursor for carbon fiber production, including high carbon content and preexisting molecular orientation in the fiber prior to carbonization. Composite fibers of regenerated cellulose and lignin (Bengtsson, Bengtsson, Sedin, & Sjöholm, 2019; Bengtsson et al., 2018; Ma et al., 2015) can provide carbon fibers with an acceptable yield (Byrne, De Silva, Ma, Sixta, & Hummel, 2018) and a life-cycle assessment by Das has shown that a lignin-based fiber is a more environmentally benign precursor alternative than PAN (Das, 2011). However, quantitative assessment of molecular orientation of cellulose–lignin composite materials is what we claim to address.

A handful of techniques have been developed to investigate molecular orientation, such as: rotor synchronized magic-angle spinning (ROSMAS) NMR spectroscopy (Gabriëlse, Gaur, & Veeman, 1996; Gabriëlse, van Well, & Veeman, 1995; Geen & Titman, 2002; Harbison & Spiess, 1985; Harbison, Vogt, & Spiess, 1986; Henrichs, 1987; Schreiber, Veeman, Gabriëlse, & Arnauts, 1999; Song et al., 1997; Svenningsson, Sparrman, Bialik, Bernin, & Nordstierna, 2019; Titman, de Lacroix, & Spiess, 1993; Tzou, Desai, Abhiraman, & Huang, 1995; Wilhelm, de Lacroix, Titman, Schmidt-Rohr, & Spies, 1993), DECODER NMR spectroscopy (Chmelka, Schmidt-Rohr, & Spiess, 1993; Schmidt-Rohr, Hehn, Schaefer, & Spiess, 1992), X-ray scattering (Hermans, Hermans, & Weidinger, 1946; Krässig, 1993; Lafrance, Pézolet, & Prud'homme, 1991; Northolt et al., 2001; Wanasekara et al., 2016), polarized Raman spectroscopy (Bower, 1972; Citra, Chase, Ikeda, & Gardner, 1995; Frisk, Ikeda, Chase, & Rabolt, 2004; Richard-Lacroix & Pellerin, 2013;

* Corresponding author at: Department of Chemistry and Chemical Engineering, Chalmers University of Technology, Göteborg, Sweden.
E-mail address: lars.evenas@chalmers.se (L. Evenäs).

https://doi.org/10.1016/j.carbpol.2020.117293
Received 19 February 2020; Received in revised form 12 October 2020; Accepted 19 October 2020
Available online 8 November 2020

Svenningsson, Lin, Karlsson, Martinelli, & Nordstierna, 2019; Yang & Michielsen, 2002, 2003), birefringence (Dawkins, 1983; Northolt et al., 2001), and infrared dichroism (Ward, 1997). The experimentally measured molecular orientation can potentially be obscured by chemical modification or composite additives for which a plethora of selected methods can be used to avoid pitfalls. This work accrues on previous investigation on regenerated cellulose by Svenningsson, Sparrman, et al. (2019), where ROSMAS solid-state NMR spectroscopy and wide angle X-ray scattering (WAXS) were used to determine the molecular orientation in comparison to polarized Raman spectroscopy Svenningsson, Lin, et al. (2019). The excellent chemical selectivity of NMR spectroscopy and ability to filter out non-oriented signals, motivates its use here. The results are also compared to WAXS and birefringence measurements.

Previous studies have reported lignin-based carbon fibers produced with wet-, dry-, and melt-spinning (Baker & Rials, 2013; Bengtsson et al., 2018; Zhang & Ogale, 2014). Lignin in itself can be meltspun, however the time required for stabilization of such fibres is not industrially compatible (Baker, Gallego, & Baker, 2012). If fibers are prepared from lignin blended with another polymer, wet spinning can be performed and the stabilization time can be reduced (Byrne et al., 2018; Kubo & Kadla, 2005; Liu, Chien, Newcomb, Liu, & Kumar, 2015; Liu et al., 2019).

Föllmer et al. (2019) presented a study with the ambition to induce a preferred orientation in lignin by adding graphene oxide to the spinning dope solution. They found an increased orientation with graphene oxide concentration, though they could not distinguish if lignin contributed to the anisotropy, neither could the combination of lignin and graphene oxide be used to produce continuous fibers.

The ability to perform continuous spinning and the application of a draw ratio higher than 1 are essential features to achieve high molecular orientation of a regenerated cellulose fiber (Michud, Hummel, & Sixta, 2016). The tensile modulus of a 50 wt% softwood lignin cellulose–lignin composite fiber have been reported to increase with an increased draw ratio (Bengtsson, Jedvert, Köhnke, & Theliander, 2019). However, if the enhanced modulus is solely a result of more oriented cellulose was not identified. Existence of possible oriented lignin has been reported in the secondary cell wall in wood (Atalla & Agarwal, 1985; Salmen, Olsson, Stevanic, Simonovic, & Radotic, 2011). The cause for orientation is still debated, but recent studies using DNP-NMR show that the lignin binds to xylan in a possible cellulose–xylan–lignin system (Kang et al., 2019). Is lignin, which is chemically bound to oriented hemicellulose or cellulose, acting as scaffold? Is it possible to induce any molecular orientation preference to the lignin molecules in synthetic conditions? These are both questions that concern the work herein.

2. Experimental

2.1. Materials

Softwood Kraft lignin (SKL) was received from Bäckhammar Pilot Plant (Bäckhammar, Sweden) where it was isolated with the LignoBoost method using industrial black liquor. Before use, SKL was at 60 °C at 100 mbar for 15 h and passed through a 0.5 mm sieve. A softwood Kraft dissolving pulp (DKP) with an intrinsic viscosity of 465 mL/g (measured according to ISO 5351:2010) was purchased from Georgia Pacific Cellulose. Pulp sheets were chopped, ground and dried for 15 h at 40 °C prior to dissolution. The solvent, 1-ethyl-3-methylimidazolium acetate (EMIMAc, Aldrich 95%), was used as received. A European spruce sample was obtained by turn milling a wood cylinder 45° against the wood grains.

2.2. Dissolution

Lignin and cellulose were dissolved simultaneously in neat EMIMAc at 70 °C, respectively, for 1 h in a closed reactor with overhead stirring at 30 rpm. Solutions were prepared with 8–24 wt% solid content, with 8 wt % cellulose and 0–16 wt% lignin, i.e. 0–67 wt% lignin to cellulose ratio in the solution, see Table 1 for the complete sample matrix. Complete dissolution was confirmed by observing the solutions in light microscopy, Nikon Eclipse Ci-POL (Nikon Instruments, Tokyo, Japan), using crossed polarizers. Deaeration was performed at 60 °C and below 100 mbar pressure for 15 h.

Table 1
Molecular orientation data from birefringence (Δn) WAXS (P_2), and ROSMAS NMR (P_2) from fibers with varying lignin ratio, draw ratio and solution temperature.

Sample	LR	DR	°C	Δn	WAXS P_2	NMR P_2
L0A	0%	2	40	0.042 ± 0.003	0.37 ± 0.01	0.45 ± 0.01
L0B	0%	6	40	0.042 ± 0.005	0.46 ± 0.01	–
L10A	10%	2	40	0.038 ± 0.003	0.37 ± 0.01	–
L10B	10%	6	40	0.038 ± 0.004	0.44 ± 0.01	0.43 ± 0.02
L33A	33%	2	40	0.028 ± 0.003	0.34 ± 0.01	–
L33B	33%	6	40	0.032 ± 0.003	0.39 ± 0.01	–
L50A	50%	2	40	0.020 ± 0.003	0.26 ± 0.01	–
L50B	50%	6	40	0.023 ± 0.002	0.36 ± 0.01	–
L50D	50%	2	70	0.018 ± 0.002	0.24 ± 0.01	0.35 ± 0.02
L50E	50%	6	70	0.020 ± 0.001	0.33 ± 0.01	0.41 ± 0.02
L50F	50%	10	70	0.021 ± 0.003	0.35 ± 0.01	0.41 ± 0.03
L67A	67%	2	70	0.0129 ± 0.0003	0.26 ± 0.01	–
L67B	67%	6	70	0.0149 ± 0.0004	0.33 ± 0.02	0.39 ± 0.05
L67C	67%	10	70	0.016 ± 0.001	0.36 ± 0.01	–

2.3. Rheology of solutions

The solutions were analyzed through oscillating rheometry on CS Rheometer (Bohlin Instruments, Cirencester, UK) equipped with a cone/plate-geometry (250 mm/5°) to obtain the temperature-viscosity relation for each spinning solution. Rheology measurements were used as a control to facilitate fiber spinning.

2.4. Air-gap spinning

The solution was spun using bench-scale spinning equipment, customized by RISE, consisting of a piston pump, a coagulation bath (7 L) and a take-up roll. The temperature of solution was set to either 40 or 70 °C. The spinneret had 33 orifices with a diameter of 150 μm and L/D 3. The solution was filtered through a 5 μm metal fleece filter and extruded with a fixed extrusion velocity (v_e) of 4 m/min. The extruded filaments were led via an air-gap of 1 cm into a coagulation bath of deionized water at a temperature of 2–5 °C. Take-up speed (v_t) during spinning was set to either 8, 24 or 40 m/min to achieve draw ratios of 2, 6 and 10.

2.5. Characterization of spun filaments

Tensile testing (Vibroskop/Vibrodyn, Lenzing Instruments, Austria) was performed on conditioned filaments at 20 ± 2 °C and 65 ± 3% RH with an extension rate of 20 mm/min and a gauge length of 20 mm.

Birefringence was measured with Nikon Eclipse Ci POL, polarized light microscope with a 3λ Berek compensator. The thickness of the fiber was calculated from the linear density in dtex, density of the fiber and assuming a circular cross section. The pure cellulose fibers were assumed to have a density of 1.5 g/cm^3 (Sixta et al., 2015), the density of the fibers with 67% lignin was measured with a He-pycnometer AccuPycII 1340 (Micromeritics Instrument, Norcross, USA) at room temperature. The density of fibers with other lignin ratio was thereafter calculated from a linear regression of these data. The birefringence, Δn, was calculated as the ratio between the retardation of the polarized light

for maximum darkness divided by the fiber thickness.

2.6. Solid state NMR spectroscopy

A bundle of composite cellulose–lignin fibers was spun on a flat spool with a thin layer of polystyrene glue applied between wounds. Strips were cut out at 45° angle from the fiber direction and stacked on top of each other so that it fitted a 7 mm rotor. Any additional space was filled with silicon dioxide powder for rotational stability.

NMR measurements were carried out using a Bruker 500 MHz Avance III, operating at 125.8 MHz for ^{13}C. The ROSMAS experiment was conducted on fibers at ambient temperature and 1500 Hz (±1) rotor rotation rate to sufficiently separate a few C1 sidebands from other signals. The t_1 rotor period was divided in 10 equal steps before initiating a cross polarization sequence with a constant ^{13}C rf strength of 31.25 kHz while 1H rf was ramped from 63 to 120 kHz with SPINAL64 50 kHz proton decoupling averaged over 512, 1024 and 2048 scans for each phase step. A recycle delay of 2 s, cross-polarization time of 1.5 ms and acquisition time of 20.27 ms were applied with the ^{13}C chemical shift externally referenced against adamantane. The European spruce wood cylinder was analyzed with the same settings at 4000 Hz (±1) rotation rate and averaged over 3200 scans for each phase step. 4000 Hz is beneficial for analysing the CSA of aromatic groups and 1500 Hz is better for quantitative determination of cellulose orientation on a 500 MHz magnet. The quantitative data analysis method of the 2D ROSMAS spectrum on regenerated cellulose is used as by Svenningsson, Sparrman, et al. (2019) The method describes how the nuclear magnetic chemical shift anisotropy tensor (CSA) affects the recorded signal depending on molecular orientation in the rotor and MAS rotation speed. By applying the Legendre polynomial orientation distribution function (ODF), it is possible calculate the order parameters for a linear set of calculated sub spectra and the measured experimental data with Eq. (1). A background subtraction was performed, as described in the *Supporting Information*:

$$\left(I_{M,N}\right)_{\mathrm{exp}} = \sum_{\ell=0}^{\infty} \langle P_\ell \rangle \left(I_{\ell,M,N}\right)_{\mathrm{calc}} \tag{1}$$

Regenerated cellulose produced by ionic liquids contains the cellulose II crystalline structure, which comprise of two magnetically nonequivalent anti-parallel 180° helical chains, named the Origin chain and the Center chain. Molecular orientation analysis is performed using the experimental ROSMAS Origin chain signal and its known CSA. The cellulose II CSA was provided by Svenningsson, Sparrman, et al. (2019), which employs a DFT approach. The cellulose II CSA has also been experimentally evaluated by Hesse and Jäger (2005), combining the 2D PASS method (Antzutkin, Shekar, & Levitt, 1995) and Herzfeld–Berger analysis (Herzfeld & Berger, 1980). In the ROSMAS experiment, the rotational chemical shift sidebands are denounced as N, where $N = 0$ is the isotropic shift. Molecular orientation is expressed in the M dimension, based on the Fourier transform of the rotor phase. We use signals from $M = 0, N = 0$ and $M = 1, N = 1$ sidebands from the ROSMAS 2D spectrum to determine molecular orientation. The P_2 order parameter was calculated by directly implying a Legendre polynomial orientation distribution, calculating linear solution with Eq. (1). In addition, similar P_2 order parameter values was obtained by exchanging the Legendre Polynomial ODF with the wrapped Lorentzian ODF and sequentially converting the calculated wrapped Lorentzian ODF solution to an order parameter.

2.7. Wide angle X-ray scattering

A wide angle X-ray scattering measurement was performed on fiber bundles at Chalmers University of Technology with a 0.9 mm beam diameter Rigaku 003+ high brilliance microfocus Cu-radiation source at 130 mm distance with the sample irradiated over 30 min. The cellulose

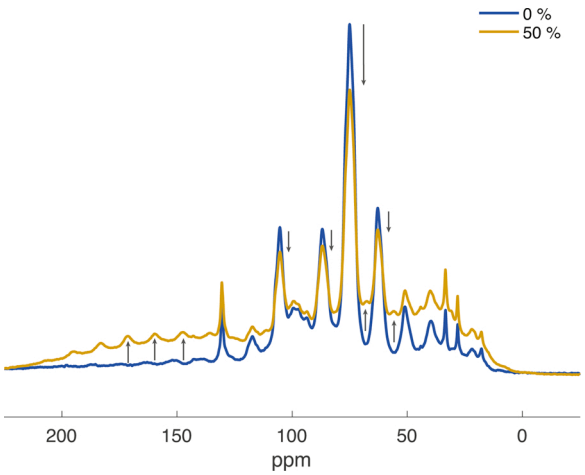

Fig. 1. CP-MAS NMR spectra at 1.5 kHz rotation rate of regenerated cellulose–lignin composite fibers with 0 and 50 wt% lignin. Increased lignin signals are shown with up arrows and decreasing cellulose signals are shown with down arrows.

Fig. 2. Photography of three cellulose–lignin fibers. Top: 67, Mid: 33, Bot: 10 wt% lignin.

II 002 azimuthal scattering signal was curve fitted simultaneously with the periodic wrapped Lorentzian function (Eq. (2)) and a flat baseline, which has shown to be a good fit for regenerated cellulose fibers (Svenningsson, Lin, et al., 2019; Svenningsson, Sparrman, et al., 2019). The curve fitting also includes a phase parameter to compensate for small miss-alignments of the fiber bundle in the sample holder:

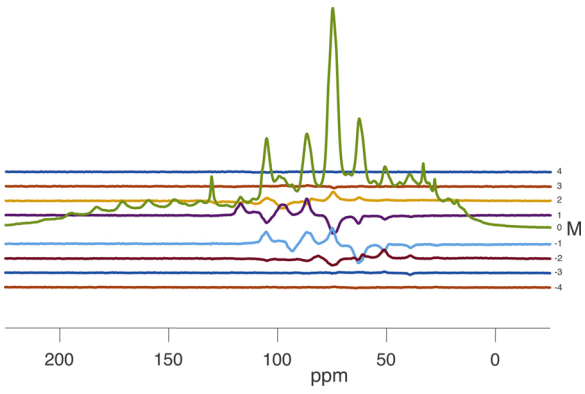

Fig. 3. ROSMAS NMR spectrum of regenerated cellulose and lignin composite fibers produced with 50 wt% lignin and draw ratio 2. Rotation rate at 1.5 kHz.

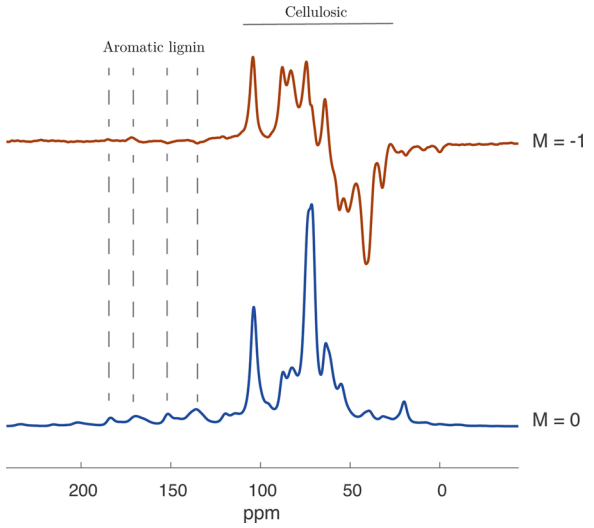

Fig. 4. ROSMAS NMR spectra of a European spruce oriented wood sample, cut at 45° from the grain direction. Rotation rate at 4 kHz. Oriented aromatic lignin seen in the 125–190 ppm region.

$$\text{wrapped Lorentzian} \quad f_{wL}(\theta) = \frac{1}{\pi} \cdot \frac{sinh\gamma}{cosh\gamma - cos2\theta} \tag{2}$$

3. Results and discussion

Fig. 1 shows CP-MAS NMR spectra at 1500 Hz rotation rate of cellulose–lignin composite fibers with 0 and 50 wt% lignin. Typical spectral features indicate the content variations of cellulose and lignin, respectively. In this work we do not study the exact cellulose–lignin ratio in the fiber. Therefore, lignin content is given from the dissolved material composition in the spinning dope solution. The lignin content in similar fibers has been previously investigated and only a minor fraction of low molecular weight lignin was found to be leached in the coagulation bath (Bengtsson et al., 2018; Bengtsson, Jedvert, Hedlund, Köhnke, & Theliander, 2019). Fig. 2 shows fibers with different lignin content, it is obvious that fibers spun from a dope with high lignin content also is much darker, i.e. contain more lignin.

Fig. 3 shows the full 2D ROSMAS spectrum of fibers produced with 50 wt% lignin and draw ratio 2. The isotropic signal, corresponding to a non-syncronized CP-MAS spectrum, is located in $M = 0$. Anisotropic signals are located in the $M \neq 0$ regions, usually characterized with significantly lower signal intensity compared to $M = 0$ signals. In Fig. 3 there are no lignin signals observed in $M \neq 0$. Considering that the aromatic lignin groups have larger chemical shift anisotropy than cellulose, which amplifies $M \neq 0$ signals in ordered materials, we may conclude that softwood kraft lignin, isolated with the LignoBoost method, is not molecularly oriented in a mechanically stretched cellulose–lignin fiber. There are however some oriented lignin signals from the 60–20 ppm region isolated in $M = \pm 2$. Signals that only show in $M = \pm 2$ are molecularly perpendicular to the rotor axis and therefore can also be attributed to the rotational forces acting on flexible components of the lignin, and therefore the finding is inconclusive. If there exists a form of lignin with long range molecular order, ROSMAS is an excellent method to detect it. A undergoing discussion suggest that some forms of lignin may have a more linear molecular structure, which could have a preferred orientation in a fiber (Awal & Sain, 2013; Crestini, Melone, Sette, & Saladino, 2011; Hosseinaei, Harper, Bozell, & Rials, 2016; Li et al., 2017; Nar et al., 2016).

The molecular orientation of the fibers, derived from wood products, is compared to native wood from spruce. The rotation rate for the wood sample is higher, at 4 kHz, to increase the aromatic signals found in lignin. Four signals from oriented lignin is observed around

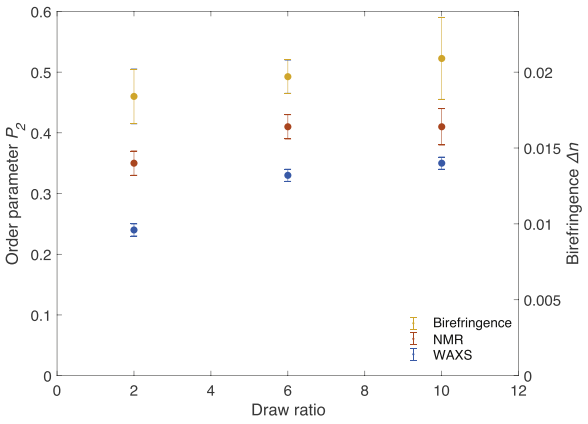

Fig. 5. Order parameter (from NMR and WAXS, left *y*-axis) and birefringence (right *y*-axis) as function of draw ratio of a cellulose–lignin fiber with 50 wt%.

125–190 ppm in $M = -1$ in a spruce solid wood sample, in addition to the oriented cellulose in Fig. 4. Atalla and Agarwal first discovered oriented lignin near the cell walls using polarized Raman spectroscopy (Atalla & Agarwal, 1985). Our study seems to confirm that some oriented aromatics from lignin in wood do occur. The ROSMAS NMR studies suggest that the oriented lignin seen in wood is not regained in a regenerated composite fiber from the same, although modified, raw materials. For example, LignoBoost extracted lignin is known to be different from native lignin. Recent work by Kang et al., published in Nature Communications, showed that lignin is bound to xylans, rather than to the cellulose itself in a cellulose–xylan–lignin system (Kang et al., 2019). Oriented lignin could be formed from the cellulose–xylan–lignin bridge, with the cellulose and hemicellulose acting as a scaffold. Our study cannot currently investigate a cellulose–xylan–lignin model since the relative amounts of xylan in dissolving pulp is much lower compared to wood. The xylan to cellulose ratio in dissolving pulp, which is used in our fibers, is 36% of the xylan to cellulose ratio of the less pure softwood kraft paper grade pulp (Bengtsson et al., 2018).

Comparable molecular orientation results from NMR, WAXS, and birefringence are shown in Fig. 5. All methods reveal an increase in molecular order with increased draw ratio in a cellulose–lignin fiber with 50 wt% lignin. The same trend of increasing molecular order was also consistent for samples where only X-ray scattering and birefringence data was available. There is a difference between the WAXS and NMR techniques with regard to what part of the material that is measured. NMR can theoretically investigate molecular orientation from both crystalline content and non-crystalline content, both of which is ordered. In this work, only the order parameters of the crystalline cellulose are reliably obtained with NMR. WAXS is usually known to be sensitive to crystalline materials, however the non-crystalline cellulose is also ordered, which may have its own different contribution. Svenningsson et al. previously found little difference in the molecular orientation of the crystalline and non-crystalline contributions in a highly oriented regenerated cellulose fiber (Svenningsson, Lin, et al., 2019; Svenningsson, Sparrman, et al., 2019). Our data suggest that the crystalline cellulose is already maximally ordered at lower stretching, while the non-crystalline material requires additional stretching to be maximally ordered.

It is practically possible to increase the draw ratio when the lignin ratio is increased while retaining continuous fiber spinning. The WAXS results in Table 1 suggest that a cellulose–lignin fiber could benefit from an increased draw ratio, in comparison to a neat cellulose fiber, in order to achieve maximal molecular order. Selecting the optimal draw ratio is important for the carbon fiber properties, which favors high molecular order in the precursor provided by the cellulose.

Table 1 shows molecular orientation in the form of P_2 order parameter from WAXS and ROSMAS with regard to lignin content, draw

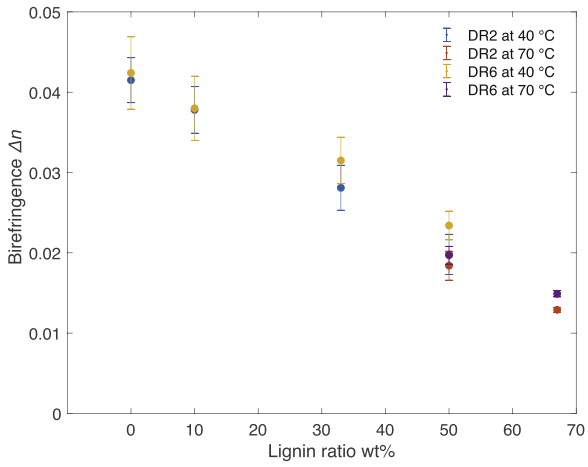

Fig. 6. Birefringence of cellulose–lignin fibers as a function of lignin content.

ratio, and dope solution temperature. Trends show decreasing orientation with increase in lignin, and also an increase in orientation with increasing draw ratio. A P_2 order parameter can in theory be calculated for birefringence, however it is challenging to correctly determine the required maximum birefringence for every new lignin blend, therefore only the birefringence values are shown (Northolt et al., 2001). Birefringence in a cellulose–lignin fiber is shown in Fig. 6 to be strongly dependent on the lignin content.

Fig. 7 shows the azimuthal plots of the regenerated cellulose–lignin fibers studied by WAXS. The normalized plots shows an orientated fiber having higher intensity around the 0° angle that coincides with the direction of the fiber. Qualitative assessments can be made on each fiber, for example: Sample L0B have a higher intensity around 0° compared to sample L0A because of the higher draw ratio of L0B.

Quantitatively, the curve represents molecular orientation distribution from the 002 reflection of the regenerated cellulose structure, fitted with a wrapped Lorentzian and a baseline. As previously noted, the 021 reflection prevents analysis of the entire range of azimuthal angles. The curve fit is therefore performed on data from ±45° azimuthal angles. It was determined with ROSMAS NMR that the lignin has no significant orientation, therefore any possible WAXS lignin signal is filtered out by

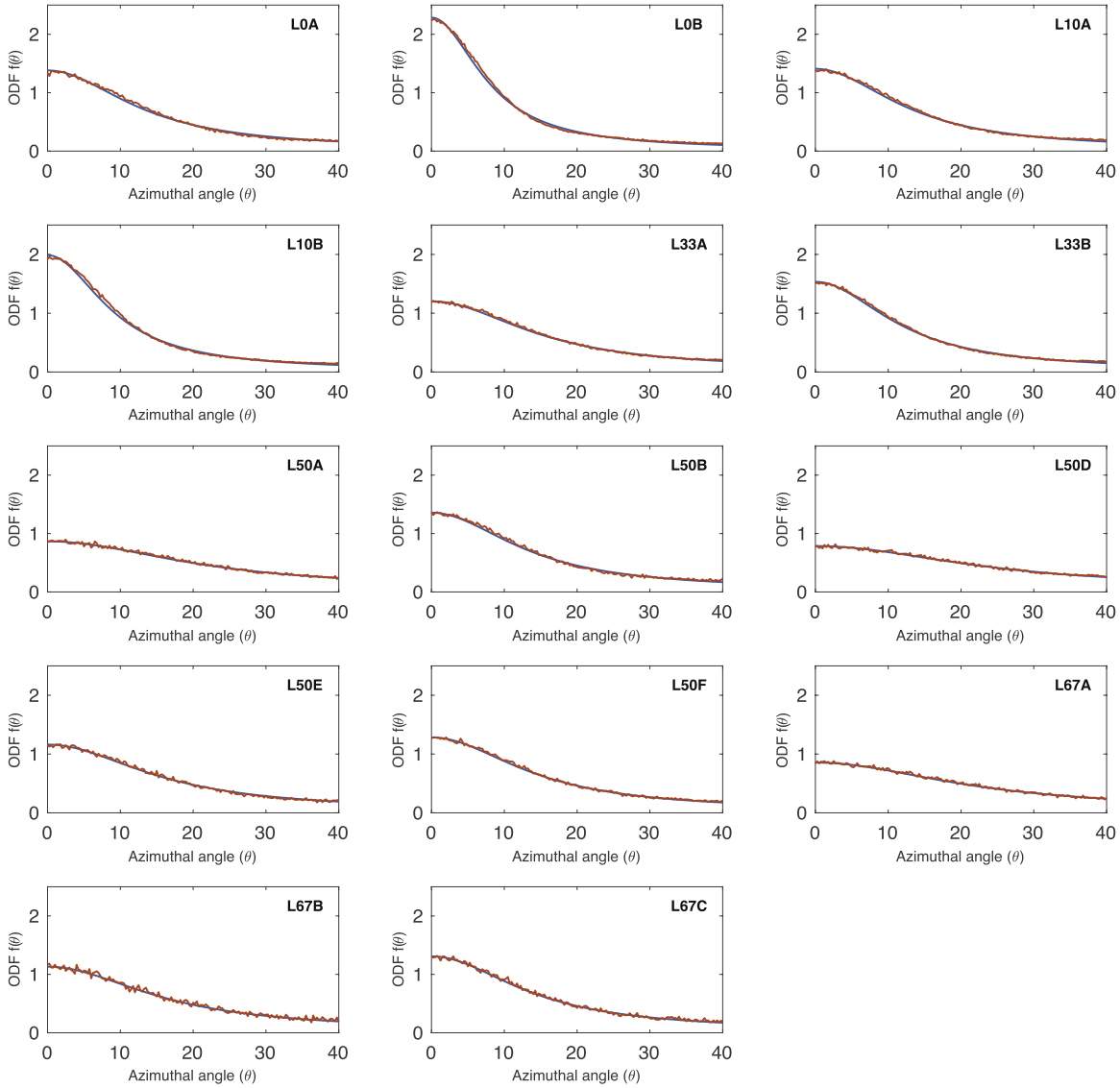

Fig. 7. WAXS azimuthal plots of the cellulose–lignin fibers. The curve represents molecular orientation distribution from the 002 reflection of the regenerated cellulose structure, fitted with a wrapped Lorentzian and a baseline. Sample names are referenced to Table 1.

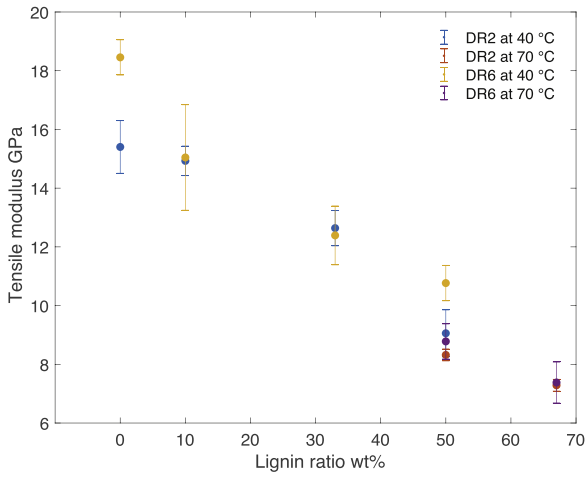

Fig. 8. Tensile modulus of cellulose–lignin fibers as a function of lignin content.

the baseline in the curve fitting procedure. Tensile modulus decreases linearly with lignin content as can be seen in Fig. 8. Studies from Ma et al. found similar results (Ma et al., 2015).

4. Conclusion

We demonstrate, with a combination of ROSMAS NMR spectroscopy and WAXS, disassociation of molecular orientation in a cellulose–lignin composite. Aromatic molecular orientation is observed in European spruce wood samples with ROSMAS NMR. The orientation of aromatic lignin in native wood is not regained in the cellulose–lignin composite fibers produced in this work. We reproduced an ionic liquid-produced cellulose–lignin composite fiber using 1-ethyl-3-methylimidazolium acetate solvent and softwood Kraft lignin. A method that bears similarities to the IONCELL strategy (Sixta et al., 2015). ROSMAS NMR spectroscopy may prove to be essential tools to predict carbon fiber materials properties from the precursor molecular composition and arrangement. Future investigations with ROSMAS NMR spectroscopy will reveal if the cellulose–xylan–lignin concept can indeed provide order of the lignin in various types of cellulose–lignin composite fibers.

Authors' contribution

Leo Svenningsson: conceptualization, methodology, software, validation, formal analysis, investigation, data curation, writing – original draft, visualization. Jenny Bengtsson: methodology, formal analysis, writing – review & editing. Kerstin Jedvert: methodology, resources, writing – review & editing, supervision. Werner Schlemmer: conceptualization, writing – review & editing. Hans Theliander: conceptualization, resources, writing – review & editing, supervision. Lars Evenäs: conceptualization, methodology, resources, writing – review & editing, supervision, project administration, funding acquisition.

Acknowledgments

This work has been carried out within the framework of the Avancell Centre for Fibre Engineering and financially supported by "Södra Skogsägarna Foundation for Research, Development and Education" and "Stiftelsen Nils och Dorthi Troëdssons forskningsfond". JB, KJ and HT gratefully acknowledge project "LightFibre" financed by Energimyndigheten. The NMR measurements were carried out at the Swedish NMR Centre, Göteborg, Sweden and at the NMR Core Facility at Umeå University, Sweden, with the assistance of Tobias Sparrman. Warm thanks to Petri Henrik Murto for handy camera work. Isabell Sarstedt is greatly acknowledged for the scientific art.

Appendix A. Supplementary data

Supplementary data associated with this article can be found, in the online version, at https://doi.org/10.1016/j.carbpol.2020.117293.

References

Antzutkin, O. N., Shekar, S. C., & Levitt, M. H. (1995). Two-dimensional sideband separation in magic-angle-spinning NMR. *Journal of Magnetic Resonance, 115*, 7–19.
Atalla, R. H., & Agarwal, U. P. (1985). Raman microprobe evidence for lignin orientation in the cell walls of native woody tissue. *Science, 227*, 636–638. https://doi.org/10.1126/science.227.4687.636
Awal, A., & Sain, M. (2013). Characterization of soda hardwood lignin and the formation of lignin fibers by melt spinning. *Journal of Applied Polymer Science, 129*, 2765–2771. https://doi.org/10.1002/app.38911
Baker, D. A., Gallego, N. C., & Baker, F. S. (2012). On the characterization and spinning of an organic-purified lignin toward the manufacture of low-cost carbon fiber. *Journal of Applied Polymer Science, 124*, 227–234. https://doi.org/10.1002/app.33596
Baker, D. A., & Rials, T. G. (2013). Recent advances in low-cost carbon fiber manufacture from lignin. *Journal of Applied Polymer Science, 130*, 713–728. https://doi.org/10.1002/app.39273
Bengtsson, A., Bengtsson, J., Olsson, C., Sedin, M., Jedvert, K., Theliander, H., et al. (2018). Improved yield of carbon fibres from cellulose and kraft lignin. *Holzforschung, 72*, 1007–1016. https://doi.org/10.1515/hf-2018-0028
Bengtsson, A., Bengtsson, J., Sedin, M., & Sjöholm, E. (2019a). Carbon fibers from lignin-cellulose precursors: Effect of stabilization conditions. *ACS Sustainable Chemistry and Engineering, 7*, 8440–8448. https://doi.org/10.1021/acssuschemeng.9b00108
Bengtsson, J., Jedvert, K., Hedlund, A., Köhnke, T., & Theliander, H. (2019b). Mass transport and yield during spinning of lignin-cellulose carbon fiber precursors. *Holzforschung, 73*, 509–516. https://doi.org/10.1515/hf-2018-0246
Bengtsson, J., Jedvert, K., Köhnke, T., & Theliander, H. (2019c). Identifying breach mechanism during air-gap spinning of lignin-cellulose ionic-liquid solutions. *Journal of Applied Polymer Science, 136*, 47800. https://doi.org/10.1002/app.47800
Bower, D. I. (1972). Investigation of molecular orientation distributions by polarized Raman scattering and polarized fluorescence. *Journal of Polymer Science Polymer Physics Edition, 10*, 2135–2153.
Byrne, N., De Silva, R., Ma, Y., Sixta, H., & Hummel, M. (2018). Enhanced stabilization of cellulose-lignin hybrid filaments for carbon fiber production. *Cellulose, 25*, 723–733. https://doi.org/10.1007/s10570-017-1579-0
Chmelka, B. F., Schmidt-Rohr, K., & Spiess, H. W. (1993). Molecular orientation distributions in poly(ethylene terephthalate) thin films and fibers from multidimensional decoder NMR spectroscopy. *Macromolecules, 26*, 2282–2296.
Citra, M. J., Chase, D. B., Ikeda, R. M., & Gardner, K. H. (1995). Molecular orientation of high-density polyethylene fibers characterized by polarized Raman spectroscopy. *Macromolecules, 28*, 4007–4012.
Crestini, C., Melone, F., Sette, M., & Saladino, R. (2011). Milled wood lignin: A linear oligomer. *Biomacromolecules, 12*, 3928–3935. https://doi.org/10.1021/bm200948r
Das, S. (2011). Life cycle assessment of carbon fiber-reinforced polymer composites. *International Journal of Life Cycle Assessment, 16*, 268–282. https://doi.org/10.1007/s11367-011-0264-z
Dawkins, J. (Ed.). (1983). *Developments in polymer characterization-4* (1st ed.). London: Applied Science Publishers.
Föllmer, M., Jestin, S., Neri, W., Derré, A., Bentaleb, A., Mercader, C., et al. (2019). Structuration of lignin-graphene oxide based carbon materials through liquid crystallinity. *Carbon, 149*, 297–306. https://doi.org/10.1016/j.carbon.2019.04.013
Frank, E., Steudle, L. M., Ingildeev, D., Spörl, J. M., & Buchmeiser, M. R. (2014). Carbon fibers: Precursor systems, processing, structure, and properties. *Angewandte Chemie International Editon, 53*, 5262–5298. https://doi.org/10.1002/anie.201306129
Frisk, S., Ikeda, R. M., Chase, D. B., & Rabolt, J. F. (2004). Determination of the molecular orientation of poly(propylene terephthalate) fibers using polarized Raman spectroscopy: A comparison of methods. *Society for Applied Spectroscopy, 58*, 279–286.
Gabriëlse, W., Gaur, H. A., & Veeman, W. S. (1996). Molecular orientation in differently processed poly(ethylene terephthalate) yarns as studied by 13C 2D CP-MAS NMR. *Macromolecules, 29*, 4125–4133.
Gabriëlse, W., van Well, H., & Veeman, W. S. (1995). Determination of the 13c magnetic shielding tensor in partially oriented polymer systems. *Solid State Nuclear Magnetic Resonance, 6*, 231–240.
Geen, C. C. N. H., & Titman, J. J. (2002). Measurement of orientation distributions using chemical shift amplification. *Solid State Nuclear Magnetic Resonance, 22*, 298–310. https://doi.org/10.1006/snmr.2002.0086
Harbison, G. S., & Spiess, H. W. (1985). Two-dimensional magic-angle-spinning nm of partially oriented systems. *Chemical Physics Letters, 124*, 128–134.
Harbison, G. S., Vogt, V. D., & Spiess, H. W. (1986). Structure and order in partially oriented solids: Characterization by 2d-magic-angle-spinning NMR. *The Journal of Chemical Physics, 86*, 1206–1218.
Henrichs, P. M. (1987). Molecular orientation and structure in solid polymers with 13C NMR: A study of biaxial films of poly(ethylene terephthalate). *Macromolecules, 20*, 2099–2112.
Herzfeld, J., & Berger, A. E. (1980). Sideband intensities in nmr spectra of samples spinning at the magic angle. *The Journal of Chemical Physics, 73*, 6021–6030. https://doi.org/10.1063/1.440136

Hesse, S., & Jäger, C. (2005). Determination of the 13c chemical shift anisotropies of cellulose i and cellulose ii. *Cellulose, 12*, 5–14.

Hosseinaei, O., Harper, D. P., Bozell, J. J., & Rials, T. G. (2016). Role of physico chemical structure of organosolv hardwood and herbaceous lignins on carbon fiber performance. *ACS Sustainable Chemistry and Engineering, 4*, 5785–5798. https://doi.org/10.1021/acssuschemeng.6b01828

Hermans, J. J., Hermans, P. H., & Weidinger, D. V. A. (1946). Quantitative evaluation of orientation in cellulose fibres from the X-ray fibre diagram. *Recueil des Travaux Chimiques des Pays-Bas, 24*, 427–447.

Kang, X., Kirui, A., Widanage, M. C. D., Mentink-Vigier, F., Cosgrove, D. J., & Wang, T. (2019). Lignin-polysaccharide interactions in plant secondary cell walls revealed by solid-state NMR. *Nature Communications, 10*, 347. https://doi.org/10.1038/s41467-018-08252-0

Krässig, H. A. (Ed.). (1993). *Cellulose: Structure, accessibility, and reactivity* (1st ed.). 1400 Yverdon, Switzerland: Gordon and Breach Science Publishers.

Kubo, S., & Kadla, J. F. (2005). Lignin-based carbon fibers: Effect of synthetic polymer blending on fiber properties. *Journal of Polymers and the Environment, 13*, 97–105. https://doi.org/10.1007/s10924-005-2941-0

Lafrance, C. P., Pézolet, M., & Prud'homme, R. E. (1991). Study of the distribution of molecular orientation in highly oriented polyethylene by X-ray diffraction. *Macromolecules, 24*, 4948–4956.

Li, Q., Xie, S., Serem, W. K., Naik, M. T., Liu, L., & Yuan, J. S. (2017). Quality carbon fibers from fractionated lignin. *Green Chemistry, 19*, 1628–1634. https://doi.org/10.1039/C6GC03555H

Liu, H. C., Chien, A. T., Newcomb, B. A., Liu, Y., & Kumar, S. (2015). Processing, structure, and properties of lignin- and cnt-incorporated polyacrylonitrile based carbon fibers. *ACS Sustainable Chemistry and Engineering, 3*, 1943–1954. https://doi.org/10.1021/acssuschemeng.5b00562

Liu, H. C., Luo, J., Chang, H., Davijani, A. A. B., Wang, P. H., & Kumar, S. (2019). Polyacrylonitrile sheath and polyacrylonitrile/lignin core bi-component carbon fiber. *Carbon, 149*, 165–172. https://doi.org/10.1016/j.carbon.2019.04.004

Ma, Y., Asaadi, S., Johansson, L. S., Ahvenainen, P., Reza, M., Alekhina, M., et al. (2015). High strength composite fibers from cellulose-lignin blends regenerated from ionic liquid solution. *ChemSusChem, 8*, 4030–4039. https://doi.org/10.1002/cssc.201501094

Mainka, H., Täger, O., Körner, E., Hilfert, L., Busse, S., Edelmann, F. T., et al. (2015). Lignin-an alternative precursor for sustainable andcost-effective automotive carbon fiber. *Journal of Materials Research and Technology, 4*, 283–296. https://doi.org/10.1016/j.jmrt.2015.03.004

Michud, A., Hummel, M., & Sixta, H. (2016). Influence of process parameters on the structure formation of man-made cellulosic fibers from ionic liquid solution. *Journal of Applied Polymer Science, 133*. https://doi.org/10.1002/app.43718

Nar, M., Rizvi, H. R., Dixon, R. A., Chen, F., Kovalcik, A., & D'Souza, N. (2016). Superior plant based carbon fibers from electrospun poly-(caffeyl alcohol) lignin. *Carbon, 103*, 372–383. https://doi.org/10.1016/j.carbon.2016.02.053

Northolt, M., Boerstoel, H., Maatman, H., Huisman, R., Veurink, J., & Elzerman, H. (2001). The structure and properties of cellulose fibres pun from an anisotropic phosphoric acid solution. *Polymer, 42*, 8249–8264.

Richard-Lacroix, M., & Pellerin, C. (2013). Accurate new method for molecular orientation quantification using polarized Raman spectroscopy. *Macromolecules, 46*, 5561–5569.

Salmen, L., Olsson, A. M., Stevanic, J., Simonovic, J., & Radotic, K. (2011). Structural organisation of the wood polymers in the wood fibre structure. *BioResources, 7*.

Schmidt-Rohr, K., Hehn, M., Schaefer, D., & Spiess, H. W. (1992). Two-dimensional nuclear magnetic resonance with sample flip for characterizing orientation distributions, and its analogy to X-ray scattering. *The Journal of Chemical Physics, 97*, 2247–2262.

Schreiber, R., Veeman, W. S., Gabriëlse, W., & Arnauts, J. (1999). Nmr investigations of orientational and structural changes in polyamide-6 yarns by drawing. *Macromolecules, 32*, 4647–4657.

Sixta, H., Michud, A., Hauru, L., Shirin Asaadi, Y. M., King, A. W., Kilpeläinen, I., et al. (2015). Ioncell-f: A high-strength regenerated cellulose fibre. *Nordic Pulp and Paper Research Journal, 30*, 43–57.

Song, Z., Antzutkin, O. N., Lee, Y. K., Shekar, S. C., Rupprecht, A., & Levitt, M. H. (1997). Conformational transitions of the phosphodiester backbone in native DNA: Two-dimensional magic-angle-spinning 31p-NMR of DNA fibers. *Biophysics Journal, 73*, 1539–1552.

Svenningsson, L., Lin, Y. C., Karlsson, M., Martinelli, A., & Nordstierna, L. (2019a). Molecular orientation distribution of regenerated cellulose fibers investigated with polarized Raman spectroscopy. *Macromolecules, 52*, 3918–3924. https://doi.org/10.1021/acs.macromol.9b00520

Svenningsson, L., Sparrman, T., Bialik, E., Bernin, D., & Nordstierna, L. (2019b). Molecular orientation distribution of regenerated cellulose fibers investigated with rotor synchronized solid state NMR spectroscopy. *Cellulose, 26*, 4681–4692. https://doi.org/10.1007/s10570-019-02430-z

Titman, J. J., de Lacroix, S. F., & Spiess, H. W. (1993). Structure and order in partially oriented solids: Characterization by 2d-magic-angle-spinning NMR. *The Journa of Chemical Physics, 98*, 3816–3826.

Tzou, D. L., Desai, P., Abhiraman, A. S., & Huang, T. H. (1995). Rotor-synchronized two-dimensional 13c cp/mas nmr studies of the orientational order of polymers 2. melt-extruded poly(ethy1ene terephthalate) fibers. *Journal of Polymer Science Part B: Polymer Physics, 33*, 63–69.

Wanasekara, N. D., Michud, A., Zhu, C., Rahatekar, S., Sixta, H., & Eichhorn, S. J. (2016). Deformation mechanisms in ionic liquid spun cellulose fibers. *Polymer, 99*, 222–230.

Ward, I. M. (Ed.). (1997). *Structure and properties of oriented polymers*. B.V: Springer-Science + Business Media.

Wilhelm, M., de Lacroix, S. F., Titman, J., Schmidt-Rohr, K., & Spies, H. (1993). The orientation distribution in an industrial sample of poly(p-phenyleneterephthalamide) determined by two- and three-dimensional NMR techniques. *Acta Polymerica, 44*, 279–284.

Yang, S., & Michielsen, S. (2002). Determination of the orientatin parameters and the raman tensor of the 998 cm^{-1} band of poly(ethylene terephthalate). *Macromolecules, 35*, 10108–10113.

Yang, S., & Michielsen, S. (2003). Orientation distribution functions obtained via polarized raman spectroscopy of poly(ethylene terephthalate) fibers. *Macromolecules, 36*, 6484–6492.

Zhang, M., & Ogale, A. A. (2014). Carbon fibers from dry-spinning of acetylated softwood kraft lignin. *Carbon, 69*, 626–629. https://doi.org/10.1016/j.carbon.2013.12.015